

## **IV. INTERFACES MODELLING UNDER CYCLIC LOADING**

### ***IV.1. MODEL DISCRPTION***

To model the behaviour of soil under cyclic solicitation, several models based on a elasto-plastic law have already been implemented. However, they still have major disadvantages that prevent their utilisation as their development:

- A long calibration. Twenty parameters are coupled to identify to identify with precision the behaviour of a given soil.
- A cumbersome. The complexity of the phenomenon, and coupling mechanisms are calculations that can extend over time and soon became prohibitive.

The Ramberg-Osgood law and Byrne law are two laws of incremental type that can store the state of the ground at each change of direction of the solicitation. This type of process is less onerous in terms of computing time and the use of this type of law has already allowed to reproduce successfully the cyclical behaviour of the soil, including the hysteresis loops and the magnitude of densification at the end of  $N$  cycles.

Both laws were originally developed to model the behaviour of soils. The purpose of this study is attempting to apply it to the interface. The main idea of this study is to begin to implement these laws and then check the consistency of the results to determine whether the inclusion of such laws only, are sufficient to model the behaviour of the interface under cyclic loading.

#### ***IV.1.1. Ramberg-Osgood's model***

The basic idea of the Ramberg-Osgood model is to use a non-linear elastic law to create a hysteresis loop under cyclic stress. This law, which the advantage of being easier on the identification of parameters with a faster computation time, must always be limited by a limit of plasticity: the criterion of Mohr-Coulomb.

The objective here is to explore the possibility of applying the Ramberg-Osgood model to model the behaviour of the interface under cyclic loading. According to Ramberg and Osgood (1943) the law is written as follows:

$$\left\{ \begin{array}{l} G = \frac{G_{\max}}{1 + \alpha \left( \frac{|\tau - \tau_c|}{m\tau_y} \right)^{r-1}} \\ K = K_{\max} \end{array} \right. \quad (4.1.1.1)$$

According to the study of analogy between interface and soil by Boulon and Nova (1990), the equivalence of this equation for an interface is:

$$\left\{ \begin{array}{l} K_s = \frac{K_{s\max}}{1 + \alpha \left( \frac{|\tau - \tau_c|}{m\tau_y} \right)^{r-1}} \\ K_n = K_{n\max} \end{array} \right. \quad (4.1.1.2)$$

Where:  $\alpha$  and  $r$  = Model parameters  
 $\tau$  = Shear stress at t  
 $\tau_c$  = Shear stress at the last peak  
 $\tau_y$  = Shear stress at yielding

$$\tau_y = \sigma_n \tan \phi_{\max}$$

We choose  $m = 1$  in the first half cycle and  $m = 2$  the rest of the time. This ensures the consistent of the model with the second law of Masing (1926): in the shear stress-deformation curve, all the curves of loading-unloading have the profile as the initial loading curve.

$K_{n\max}$  and  $K_{s\max}$  are given by the following law of Hertz:

$$\left\{ \begin{array}{l} K_{s\max} = K_{s0} \left[ \frac{\sigma_n}{\sigma_{ref}} \right]^n \\ K_{n\max} = K_{n0} \left[ \frac{\sigma_n}{\sigma_{ref}} \right]^n \end{array} \right. \quad (4.1.1.3)$$

where :  $n$  = Model parameter  
 $\sigma_{ref}$  = The reference confinement (initial normal stress = 100 kPa)  
 $K_{s0}$  = Tangential stiffness module at the reference confinement

$K_{n0}$  = Normal stiffness module at the reference confinement.

The expression of the Ramberg-Osgood law demonstrates, through  $\tau_c$ , the need to detect the structure of cycles in shear stress and to memorize the state of the interface at the last peak. A change in direction of the solicitation makes the interface shear stiffness module return to the initial value (first law of Masing, 1926 to the soil), dissociate the loading and unloading curve, and thus generate hysteresis loops.

#### **IV.1.2. The Byrne law**

The same as the adaptation of the Ramberg-Osgood law, to reconstruct the shear stress curve of the interface during cyclic loading, here we use the Byrne law, initially proposed to model the behaviour of soils, to model the normal densification (normal displacement) of the interface.

This law of hardening consist basically to observe the amplitude of each cycle or half-cycle of the deviatory deformation and deduce a variation of soil density representative of that period. But in an interface, which must be noted is the amplitude of each cycle or half-cycle of the normal displacement (see Figure 43). The latest expression of this law according to Byrne (1994), after elimination of possible sources of instability of earlier versions, is as follows:

$$\Delta \varepsilon_{1/2cycle}^v = \frac{1}{2} \gamma C_1 \exp\left(\frac{-C_2 \varepsilon_v}{\gamma}\right) \quad (4.1.2.1)$$

Where:  $\Delta \varepsilon^v$  = Volume variation associated with the period  
 $\varepsilon_v$  = Cumulative volume variation at the last cycle  
 $\gamma$  = Amplitude of the deviatory deformation at the 1/2 cycle  
 $C_1$  and  $C_2$  are the law's parameters

And equivalence for an interface is as follows

$$\Delta u_n^{irr} / 2_{cycle} = \frac{1}{2} \gamma C_1 \exp\left(\frac{-C_2 u_n}{\gamma}\right) \quad (4.1.2.2)$$

Where:  $\Delta u_n^{irr}$  = Normal displacement increment or variation  
 $u_n$  = Cumulative normal displacement at the last hysteresis loop  
 $\gamma$  = Amplitude of the tangential displacement at  $\frac{1}{2}$  loop

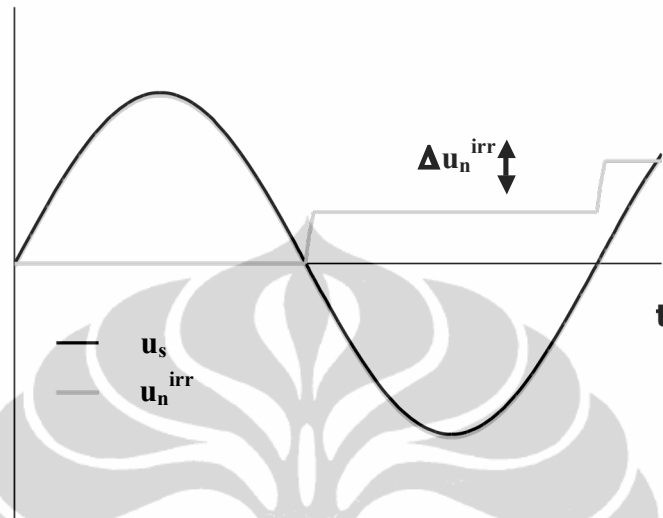


**Figure 43. Injection of the variations of the normal displacement due to the cyclic phenomena**

The injection of this variation only in the simulation for each half cycle, it is not sufficient to simulate the complete behaviour of the interface in terms of density, but it gives a good estimate of the total amplitude of densification at the end of N cycles

## **IV.2. IDENTIFICATION OF THE MODEL PARAMETERS**

To model the behaviour of the interface under cyclic loading using the Ramberg-Osgood and Byrne laws, it is therefore necessary to define seven parameters:  $k_n$ ,  $k_s$ ,  $C_1$ ,  $C_2$ ,  $\alpha$ ,  $r$  and  $\phi_{max}$ . Three of them have already been defined in the monotone modelling. Consequently, only four parameters that are specific to the cyclical behaviour of the interface that have to be defined.

### **IV.2.1. Ramberg-Osgood parameters**

The parameters of the Ramberg-Osgood model must be manipulated to achieve the best possible match between the shear stress curve in the simulation and experimental way. The parameter  $r$  controls the magnitude of the shear stiffness modulus for each change of direction of the sollicitation. Figure 44 shows the influence

of this parameter. The second parameter,  $\alpha$ , is used to control the magnitude of the non-linearity factor of the shear stress curve. His influence on the simulation is shown in Figure 45.

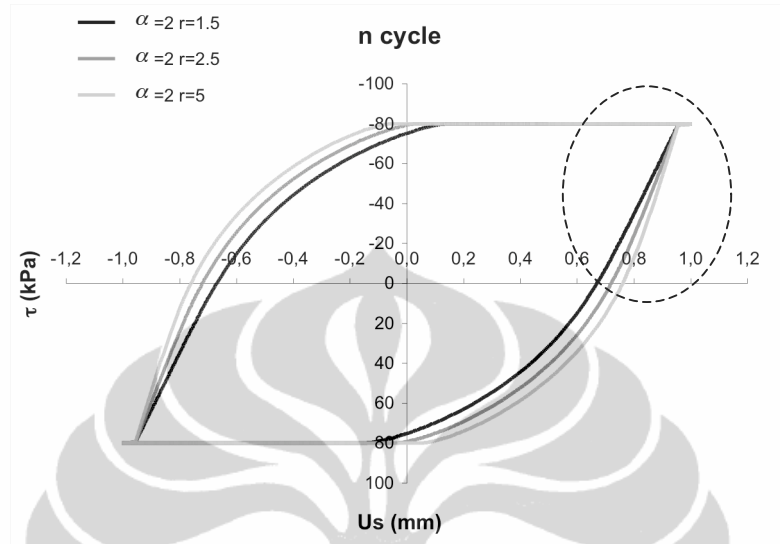


**Figure 44. Influence of  $r$**

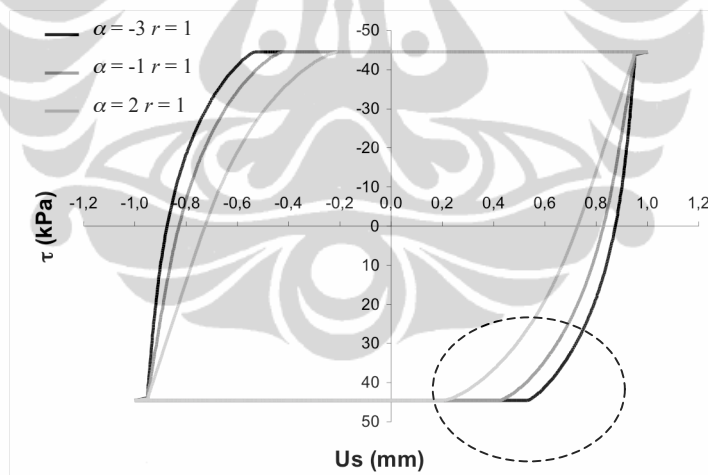


**Figure 45. Influence of  $\alpha$**

#### **IV.2.2. Byrne's parameters**

The two parameters of the Byrne law,  $C_1$  and  $C_2$ , make it possible to estimate the densification of interface at the end of each  $N / 2$  cycle. These parameters can be calibrated from the CNL experimental results.

To make a first estimation of these parameters, a calibration on the experimental displacement curve can be achieved. Figures 46 and 47 show the normal

displacement curve of a rough interface with dense sand in function of the number of cycles  $N$ . From this figure, several curves of the Byrne function can be superposed to find the best set of parameters.

Through these two curves, it may be noted that the parameter  $C_1$ , control specifically the slope of the normal displacement increment at the beginning of loading (see Figure 46). And  $C_2$  control the magnitude of the nonlinear behaviour of the normal displacement after a certain  $n =$  number of cycles (see Figure 47).

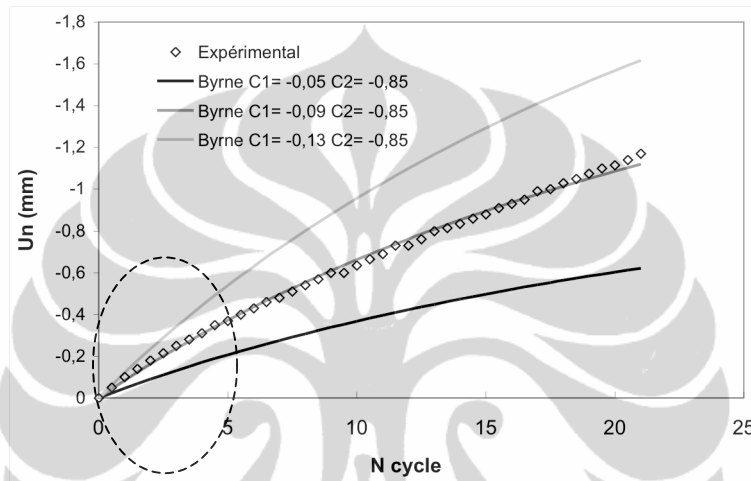


**Figure 46.** Byrne's parameters determination– Influence of  $C_1$

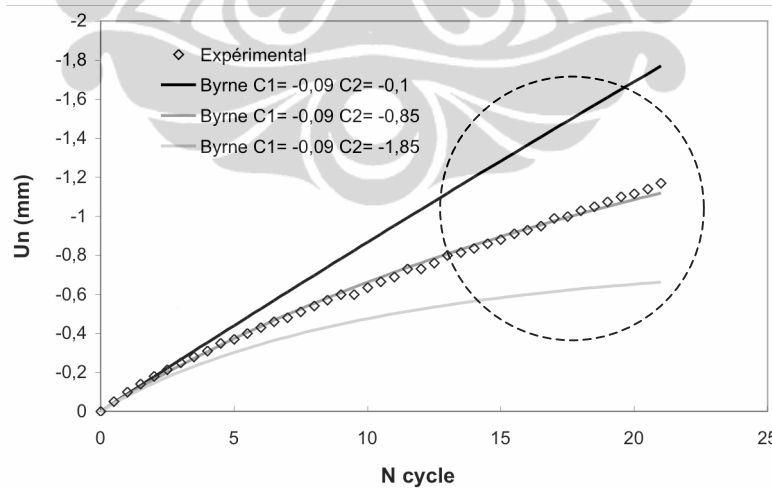
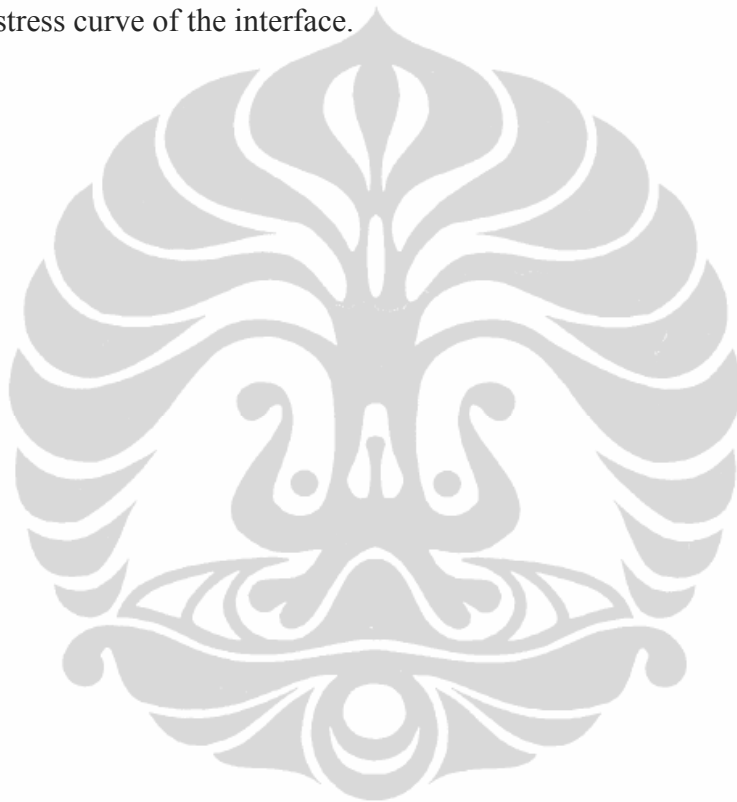


**Figure 47.** Byrne's parameters determination– Influence of  $C_2$

### ***IV.3. PARTIAL CONCLUSION***

Unlike the modelling of the interface in a monotone solicitation, the objective of this chapter was not to introduce a new model constitutive, but to validate a model of shear stress and displacement incremental, which have already been applied to the modelling of soil behaviour, in an interface modelling.

Both models tested here are incremental models that are independent of each other. When tested at a constant normal stress, the parameters influence only the model where it belongs. However, in a cyclic test at a zero normal displacement, the law Byrne may also influence the shear stress curve of the interface.



## V. IMPLEMENTATION ON FLAC

The present work following the work carried out by Riyono (2005), implementation will be carried out under the FLAC software, he had already used. The method and calculation models used by FLAC will be briefly explained below before detailing the various important issues in the implementation.

### V.1. *FLAC ARCHITECTURE*

FLAC is a software finite difference calculation. It uses a cycle of resolution to move towards a balance in a static simulation and calculate approximate rapidly changing dynamics. The resolution method is called incremental, every step of calculation, a cycle is complete resolution traveled and external actions are updated if necessary (in dynamics, no time will be substantially less than the evolution external actions for the calculation to be meaningful). The resolution cycle of the software is given in figure 48.

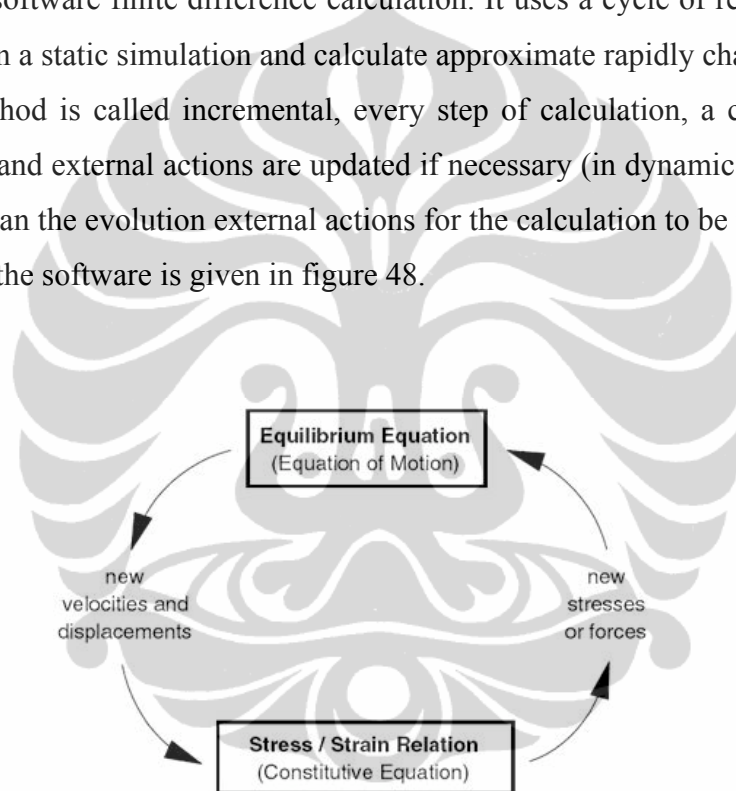


**Figure 48. Basic explicit calculation cycle [ITASCA 2005]**

The cycle consists of two blocks of equations. On the one hand there are the equations of balance inherent in the physical, and therefore can not be altered, which can deduct the deformation based on internal and external constraints in the system. On the other hand are the constitutive equations of the model, which ensures calculating deformation forced to assign to newly calculated. Only on the second block a user FLAC may intervene in defining a new Constitution, so therefore on this block is where this work occurs.



*FLAC* uses a contact logic, which is similar in nature to that employed in the distinct element method, for either side of the interface (e.g., Cundall and Hart 1992). The code keeps a list of the gridpoints ( $i, j$ ) that lie on each side of any particular surface. Each point is taken in turn and checked for contact with its closest neighboring point on the opposite side of the interface. Referring to Figure 4.1, gridpoint  $N$  is checked for contact on the segment between gridpoints  $M$  and  $P$ . If contact is detected, the normal vector,  $\mathbf{n}$ , to the contact gridpoint,  $N$ , is computed. A “length,”  $L$ , is also defined for the contact at  $N$  along the interface. This length is equal to half the distance to the nearest gridpoint to the left of  $N$  plus half the distance to the nearest gridpoint to the right, irrespective of whether the neighboring gridpoint is on the same side of the interface or on the opposite side of  $N$ . In this way, the entire interface is divided into contiguous segments, each controlled by a gridpoint.

During each timestep, the velocity  $\dot{u}_i$ , of each gridpoint is determined. Since the units of velocity are displacement per timestep, and the calculational timestep has been scaled to unity to speed convergence (see ITASCA 2005), then the incremental displacement for any given timestep is:

$$\Delta u_i \equiv \dot{u}_i \quad (5.2.1)$$

The incremental relative displacement vector at the contact point is resolved into the normal and shear directions, and total normal and shear forces are determined by:

$$F_n^{(t+\Delta t)} = F_n^{(t)} - k_n \Delta u_n^{(+\frac{1}{2})\Delta t} L \quad (5.2.2)$$

$$F_s^{(t+\Delta t)} = F_s^{(t)} - k_s \Delta u_s^{(+\frac{1}{2})\Delta t} L \quad (5.2.3)$$

where  $k_n$  and  $k_s$  are respectively the normal and shear stiffness module.

To model an interface, *FLAC* offers two types of model: (a) an interface that is stiff enough compared to the surrounding material, but which can slip and perhaps open in response to the anticipated loading; or (b) an interface that is soft enough to influence the behaviour of the system. In the latter case, properties should be derived from tests on real joints (suitably scaled to account for size effect), or from published data on materials similar to the material being modeled. To model the interface as close as possible as the real one, these last model were chosen.

To set the normal modulus,  $k_n$ , and the shear modulus,  $k_s$  it is tempting (particularly for people familiar with finite element methods) to give a very high value for these stiffness to prevent movement on the interface. However, *FLAC* does “mass scaling” (see ITASCA 2005 section 1.3.5) based on stiffnesses — the response (and solution convergence) will be very slow if very high stiffnesses are specified. It is recommended that the lowest stiffness consistent with small interface deformation be used. A good rule-of-thumb is that  $k_n$  and  $k_s$  be set to *ten times* the equivalent stiffness of the stiffest neighbouring zone. The apparent stiffness (expressed in stress-per-distance units) of a zone in the normal direction is

$$\max \left[ \frac{\left( K + \frac{4}{3} G \right)}{\Delta z_{\min}} \right] \quad (5.2.4)$$

Where  $K$  &  $G$  are the bulk and shear modulus, respectively; and  $\Delta z_{\min}$  is the smallest width of an adjoining zone in the normal direction. The  $\max [ ]$  notation indicates that the maximum value over all zones adjacent to the interface is to be used.

If the physical normal and shear stiffness are less than ten times the equivalent stiffness of adjacent zones, then there is no problem in using physical values. If the ratio is much more than ten, the solution time will be significantly longer than for the case in which the ratio is limited to ten, without much change in the behaviour of the system. Serious consideration should be given to reducing supplied values of normal and shear stiffness to improve solution efficiency. There may also be problems with interpenetration if the normal stiffness,  $k_n$ , is very low. A rough estimate should be made of the joint normal displacement that would result from the application of typical stresses in the system ( $u = \sigma / k_n$ ). This displacement should be small compared to a typical zone size. If it is greater than, say, 10% of an adjacent zone size, then there is either an error in one of the numbers or the stiffness should be increased if calculations are to be done in large-strain mode.

All these properties are deducted from the laboratory testing (e.g., shear test and triaxial test). These tests can give us some physical properties such as friction angle of the interface, the cohesion throughout the interface, the dilatancy angle, tensile strength, and the normal and shear stiffness modulus.

The structure containing these values and results of the interface calculation of *FLAC* can be accessed and manipulated, by using a programming language, *FISH*. The pointer to these data structures is provided in a form of scalar variables *FISH*. These files have the

extension .FIN (Fish include file), they provide symbolic names for sizes, compensation and the numerical values. The files (. FIN) served two purposes: first, they record the significance of different data elements, and secondly, the files can be called from a data file, where they are automatically defined and executed on the appropriate symbol. The .FIN which stores data structures interface FLAC is "INT.FIN." This file is provided in Appendix H.

### ***V.3. DIRECT SHEAR STRESS MODELISATION IN FLAC***

The interface modelling is done easily with the interface tools on FLAC. The definition of material, mesh size and declaration of the interface are the early stages of the modelling. The following important point to be defined is the boundary conditions. As presented in Chapter II, there are three types of boundary conditions, which are often used in shear test. In this study, only two of these types will be used, the CNL test and the CNV test.

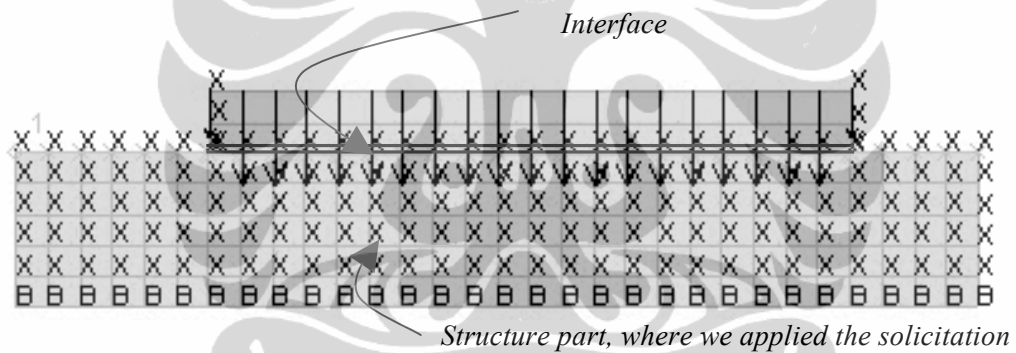


**Figure 50. Interface modelling for a CNL test**

Figures 50 and 51 are the mesh model. Figure 50 shows the model for a CNL test, which is done first by defining the boundary conditions, before setting a constant confinement load throughout the test. The modelling of a CNV test, described in Figure 51, was made by applying first the boundary conditions on the lower part of the structure, followed by a initial confinement load, and then completed by fixing the upper part of the system (the soil).

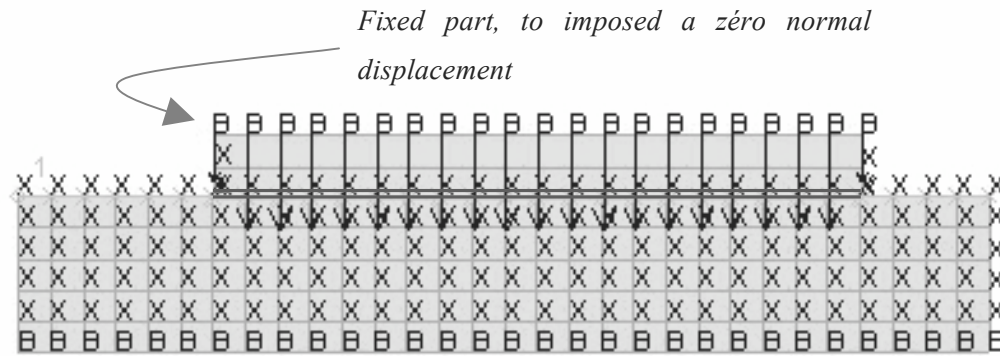


**Figure 51. Interface modelling for a CNV test**

#### ***V.4. MONOTONE MODEL STRUCTURE***

To work on the behaviour of the interface, as discussed above, the variables in the data structure must be collected before storing it in another area calculation. For this model, the calculations to simulate the interface principal stress and the interface displacement, follows the flow chart diagram shown in Figure 52.

The modification of the interface parameters are done through the programming language FISH. The initial parameters are stored and the changes are recorded through a programming language, which are then taken into account in internal calculation of the interface on FLAC.

Some details of implementation that the author considers important and complex will be defined in the following sub-chapters.

#### ***V.5. STRUCTURE DU MODÈLE CYCLIQUE***

The modelling of a cyclic test is based on the algorithm of a monotonic test. In order to implement an alternating solicitation, there are three methods that can be made depending on the type of solicitation given. For a solicitation with function type or frequency response of an earthquake, we could use the FLAC version dynamic, which allows you to specify the solicitation directly. For a solicitation controlled by a constant limit, the static version of FLAC can be used; the change of the direction of solicitation is done whenever the limit is crossed.

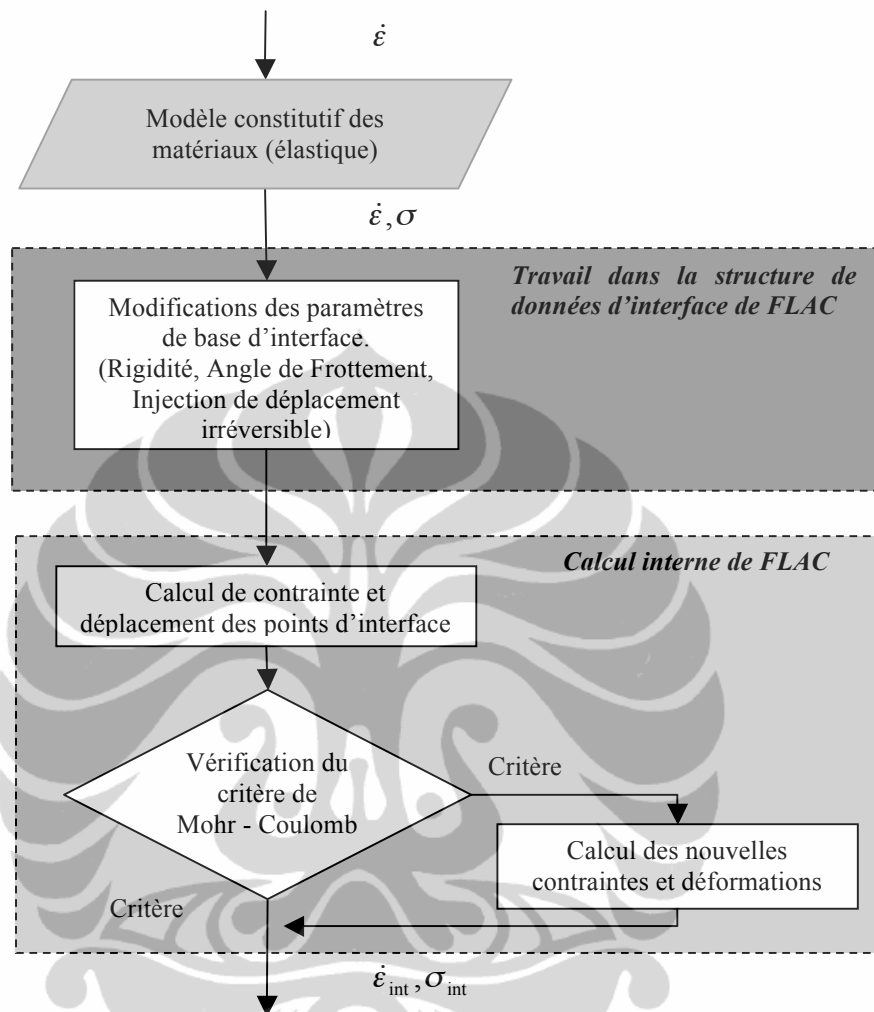


Figure 52. General flow chart for interface calculation

In this study, the simulation of cyclic loading was conducted under a CNL direct shear test controlled by a value of tangential displacement. This type of solicitation matches with the static solution with a value  $u_s$ , which showing the end of a cycle (the peak of the loop). Figure 53 shows the simplified algorithm for a cyclic solicitation used in this study.

### V.6. PEAK VALUE DETECTION

Modelling the interface behaviour during a cyclic loading, demonstrates, through the Ramberg-Osgood model, the need to detect the structure of cycles of the shear stress response and to memorize the state of the interface at the last peak. Similarly, the injection of the

irreversible normal displacement by Byrne's law reflects the need to detect the structure of the normal displacement cycles and to remember the state of the interface at the last peak. The model developed should therefore be able, first, to realize the detection of the structure of hysteresis cycles for both, the shear stress curve and for the normal displacement curve. The algorithm in Figure 54 shows the flow-chart of the peak detection on the shear stress curve. For the detection of the normal displacement peak, the information used will be  $u_n$  and  $u_s$ , and the axe to be cross will be the vertical displacement curve ( $u_n$ ).

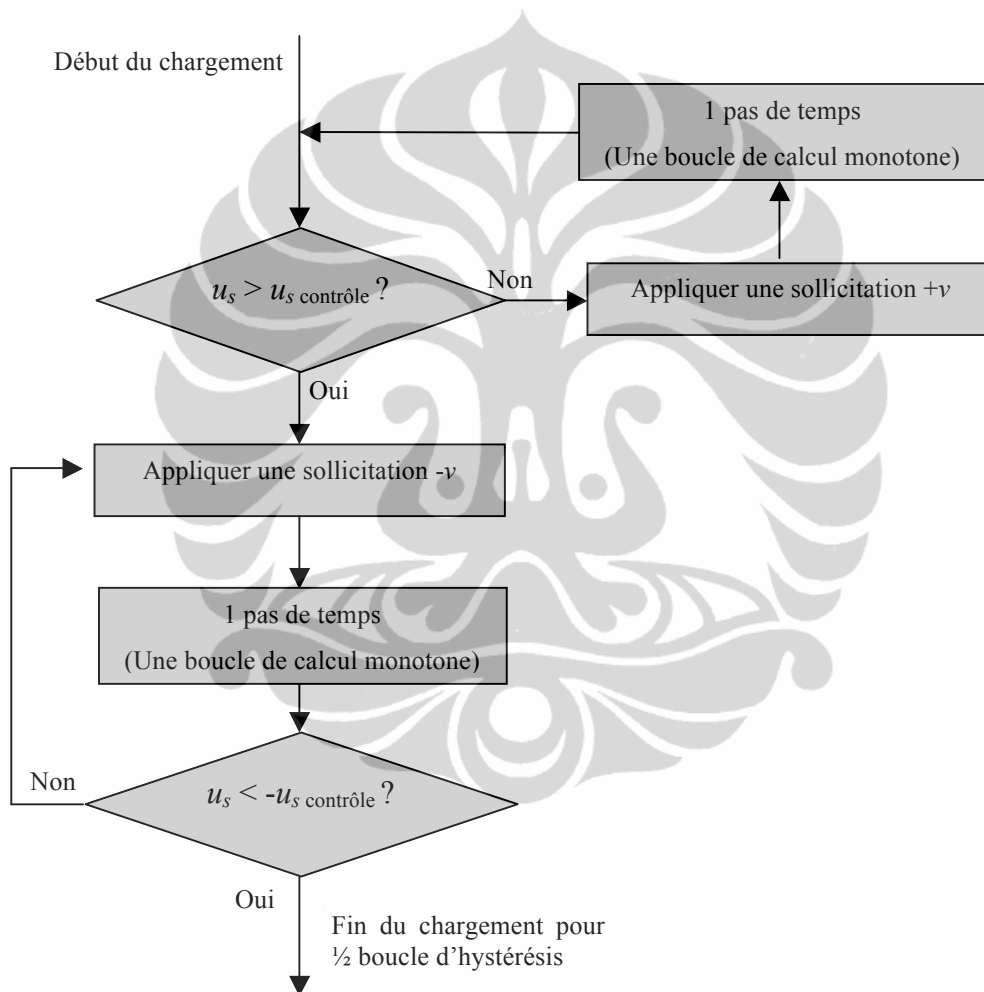


**Figure 53. The cyclic model algorithm for a 1/2 hysteric boucle**

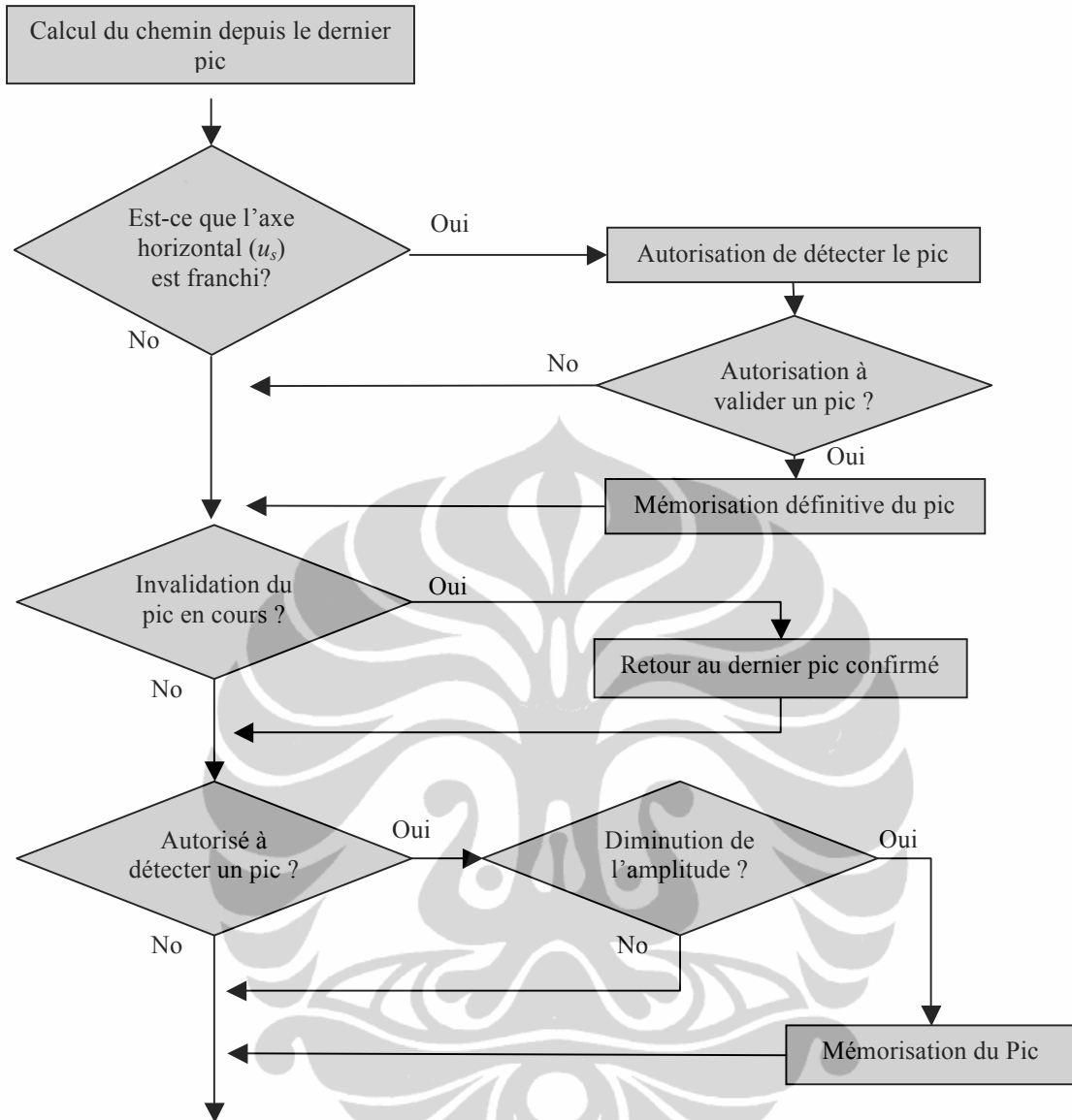


Figure 54. Flow-chart of the interface calculation procedure

### V.7. PARTIAL CONCLUSION

FLAC software already has its own methods of calculation and provides a program to define an interface. The model implementation requires the use of the Mohr-Coulomb law, which therefore limits the possibility of modelling the interface behaviour. In addition, the architecture of calculations on FLAC for an interface requires the use of pointers and data modification from the address memory.

## VI. RESULTATS

The model parameters used in these simulations are based in part on the laboratory experiment of a Hostun sand, and partly from the experimental test conducted on soil-structure interface involving the same type of material. There are many studies that are dedicated to studying the behaviour of the sand (Mohkam 1983; Jafarzadeh, Javaheri, Sadek and Wood, 2008). Table 2 summarizes the characteristic values founded in these studies.

**Table 2. Physical parameters of sand Hostun**

$D_{50}$	$e_{min}$	$e_{max}$	$G_s$	$\phi_{max}$	
				Dense	Loose
0,35 mm	0.656	1.00	2.65	38 à 41°	33 à 35°

Regarding the parameters of the interface behaviour modeling, the experimental test in a shear box on the Hostun sand, were presented by Shahrouz and Rezaie (1997). According to the results of these tests, we could deduced the maximum friction angle,  $\phi_{max}$  of the interface (see Table 3).

**Table 3. Maximum friction angle of soil-structure interface [Shahrouz and Rezaie, 1997]**

Interface type	Dense sand ( $ID = 90\%$ )	Loose sand ( $ID = 15\%$ )
Rough	38.5-40°	30-32°
Smooth	28-30°	22-24°

The values of the maximum friction angle for a rough interface approach in fact those for Hostun sand ( $(\phi_{max} = 38$  to  $41^\circ$  for the dense sand and  $33$  to  $35^\circ$  for loose sand). For a smooth interface, these values are around 75% of the value for the sand.

We have therefore four variables to be carry out from a direct shear test during a solicitation monotone, seven parameters to be determined to simulate a monotonic sollicitation, and plus four other parameters to simulate the interface behaviour on a cyclic loading. Six of them are the basic parameters of the interface and are independent of modeling. Table 4 summarizes these.

Table 4. Basic data of the interface

Interface type: Sand type :	Rough		Smooth		Note
	Dense	Loose	Dense	Loose	
1 $D50$ (mm)			0,35		Mohkam (1983)
2 $Kn$ (Kpa/mm <sup>2</sup> )	800	500	800	500	Shahrour & Rezaie (1997)
3 $Ks$ (Kpa/mm <sup>2</sup> )	500	400	500	400	Shahrour & Rezaie (1997)
4 $\phi$ residual	34,3	32	29	24	Deducted from Shahrour & Rezaie (1997)

### VI.1. RÉSULTATS DE LA SIMULATION D'UN ESSAI MONOTONE

The list of parameters used in the monotonic simulation on an interface is given in Table 5.

Table 5. Monotone model parameters

Interface type: Sand type:	Rough		Smooth		Note
	Dense	Loose	Dense	Loose	
5 $\phi$ characteristics	29	32	23	24	Deducted from Shahrour & Rezaie (1997)
6 $\phi$ maximum	40	32	30	24	Deducted from Shahrour & Rezaie (1997)
Elastic non-linear parameters model					
7 $a1$	0,4	1,8	0,3	1,4	Control the non-linéarité of the shear stress curve
8 $n$	0,65	1	1	1,3	Normalize the initial normal stress (HERTZ law)
Shear stress softening parameters model					
9 $a2$	2,5	2,5	2,5	2,5	Control the softening speed of the material
10 $b$	4	4	1,6	1,6	Control the speed to reach the maximum resistance state
Dilatancy parameter model					
11 $\beta$	0,4	0,7	0,5	1	

#### VI.1.1. Rough interface with a dense sand

Based on the assumption of similarity of behaviour between a rough interface with a dense sand and soil, some of this type parameters can be deducted from the studies already carried out on the soil (or sand). Dufour-Laridan (2001) conducted triaxial tests on Hostun sand. In particular, they verified that the dependence of the shear stress curve with the average normal stress was modeled by the Hertz law with a power  $n$  of about 0.6. The model parameter  $n$ , which controle the elasticity nonlinear for this type of interface has been based on this study.

Figures 55 and 56 respectively presents the results of the simulation: the displacement curve and stress ratio curve. They were derived from a simulation with a set of parameters that represent the best behaviour of the interface, in general, for all value of initial confinement. However, the displacement curves of simulations with different parameter values, shows that there is instead a dependency of the characteristic stateparameter  $\phi_{car}$ , with the initial confinement. The simulations show that this can vary from 26 to 30° for an initial confinement from 100 to 300 kPa (see Appendix C).

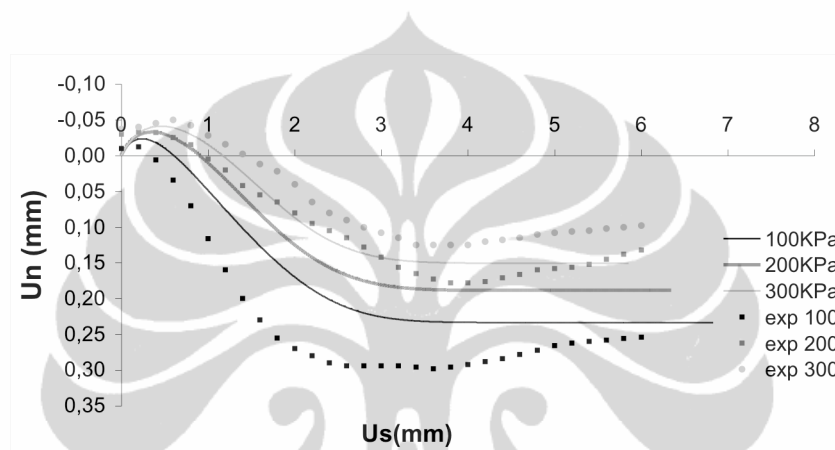


**Figure 55. Result of the simulation for a rough interface and a dense sand (ID=90%) : Displacement curve**

Regarding the stress ratio curve, the developed model coincides well with the experimental results, particularly for the simulation at  $\sigma_n = 100$  kPa. Nevertheless, the differences occurs at the beginning of loading at 200 and 300 kPa, indicates that the model probably does not adequately normalize the tangential stiffness,  $k_s$  (through the Hertz law). Even if this assumption is not consistent with the hypothesis of similarity between the behaviour of an interface rough-dense sand and soil, another simulation with a higher power of Hertz law ( $n$ ) has nevertheless been achieved (see appendix D). The result of this simulation confirms that, the value of  $n$  chosen because its augmentation influence only a little bit the shear stress ratio curve, and it indicates also an abnormality on the experimental results. The assumption of similarity is therefore still confirmed. However, the shear stress curve (see appendix B) indicates that there is indeed a disagreement in the experimental results between the test at  $\sigma_n = 200$  kPa and others.

Moreover, in figure 56, it is revealed that the stress ratio of the experimental test at  $\sigma_n = 300\text{kPa}$  is more rigid than the test at  $\sigma_n = 200\text{kPa}$ . This indicates a disagreement with the hypothesis of Evgin and Fakharian (1996), which notes that the value of the ratio requirements should be normally higher for a lower initial confinement.

These two observations remain suspended because they indicate a general question on both, the proposed model and the experimental results from which the model was built. Another simulation on a different series of experimental test would be favorable.

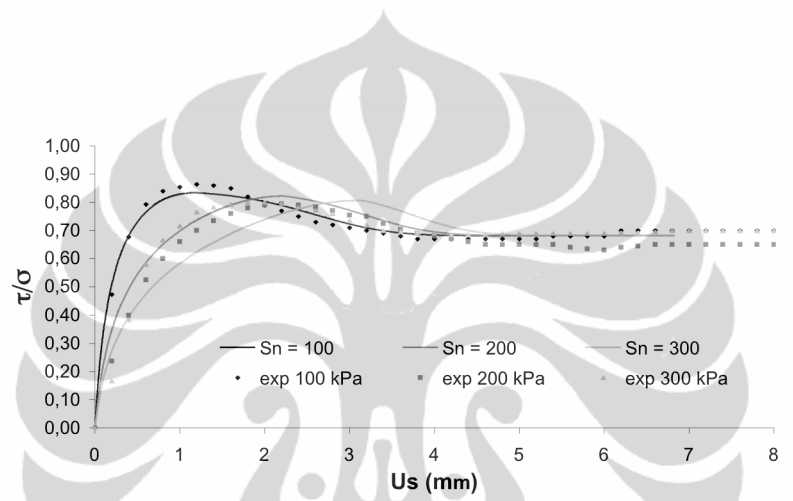


**Figure 56. Result of the simulation for a rough interface and a dense sand (ID=90%) : Stress ratio curve**

### **VI.1.2. Rough interface and loose sand**

The results of the simulation for a rough interface with loose sand are shown in Figures 57 and 58. The stress ratio of this simulation are well superposed with the experimental results and justify the set of parameters chosen for the two models: the model of nonlinear elasticity and shear stress softening.

However, in the displacement curve, it may be noted that the proposed model are well superposed with the experimental results for short displacement (up to 2 mm), but diverge for larger displacement. This discrepancy reflects the phenomenon called second phase of contractancy.

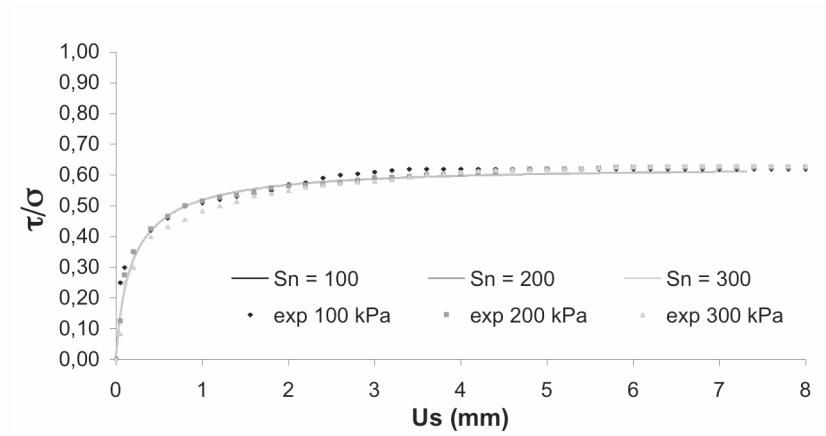


Figure 57. Result of the simulation for a rough interface and loose sand ( $ID=15\%$ ):  
stress ratio curve

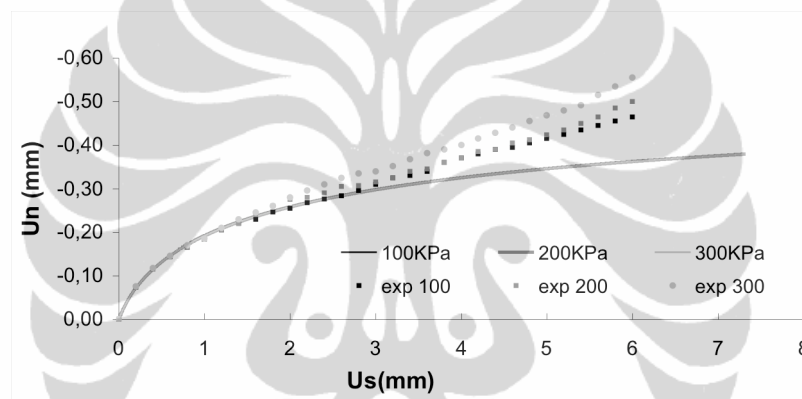


Figure 58. Result of the simulation for a rough interface and a loose sand ( $ID =15\%$ ):  
displacement curve

### VI.1.3. Smooth interface smooth and loose sand

The simulation results for a smooth interface with a dense sand are shown in Figures 59 and 60. They were carried out with a characteristics state's parameter,  $\phi_{car}$  different from that which was deduced from the experimental results. All shear stress and displacement curve correspond normally at a characteristic friction angle  $\phi_{car}=29^\circ$ , but the simulations show that this value is not appropriate (see Appendix E: the curve of movement for  $\phi_{car} = 29^\circ$ ). The value of  $\phi_{ca,r}$  which gives a better result on the displacement curve is in fact about  $23^\circ$ . These results, together with the results of simulations for a rough interface and dense sand, demonstrate the difficulty of determining the characteristic state parameter for dense materials

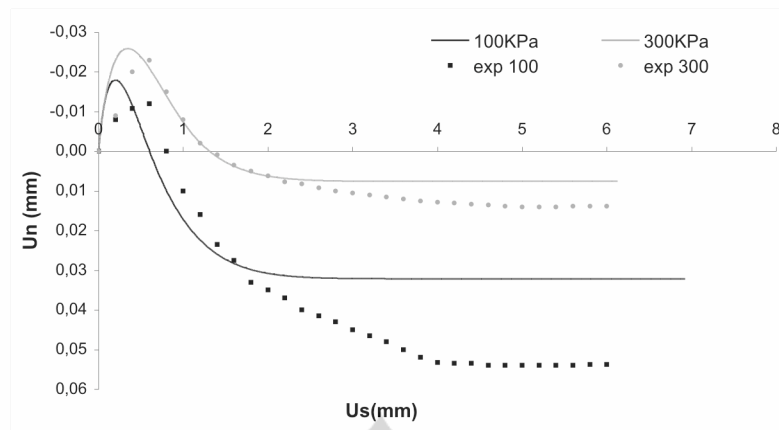


Figure 59. Result of the simulation for a smooth interface and a dense sand ( $ID=90\%$ ) : stress ratio curve

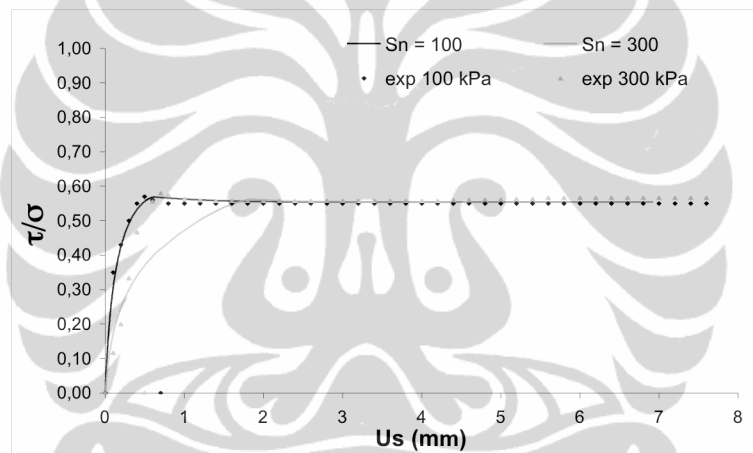


Figure 60. Result of the simulation for a smooth interface and a dense sand ( $ID=90\%$ ) : Displacement curve

Regarding the displacement curve, one can observe the same phenomenon in a rough interface with dense sand: the simulations were well superposed with the experimental result for 100 kPa, but not for the rest. We can see through the figure 60, that the model underestimates the stiffness of the interface at the beginning of the loading. However, this phenomenon is not reproduced in a case of loose sand, for which the softening model does not influence the behaviour of the interface tested. This last observation indicates that there may be a dependency on the shear stress softening model with the initial confinement.

From these results, and shear stress curve for dense sand (see Appendix B), there are small differences between the experimental's stress curve and the curve during

a simulation for a dense sand. This is probably because the maximum friction angles chosen in this study were average values for any initial constant value of confinement. This observation implies that the maximum angle of friction may slightly depended on the initial normal stress.

#### **VI.1.4. Smooth interface and loose sand**

The simulation results for a smooth interface with loose sand are shown in Figures 61 and 62.

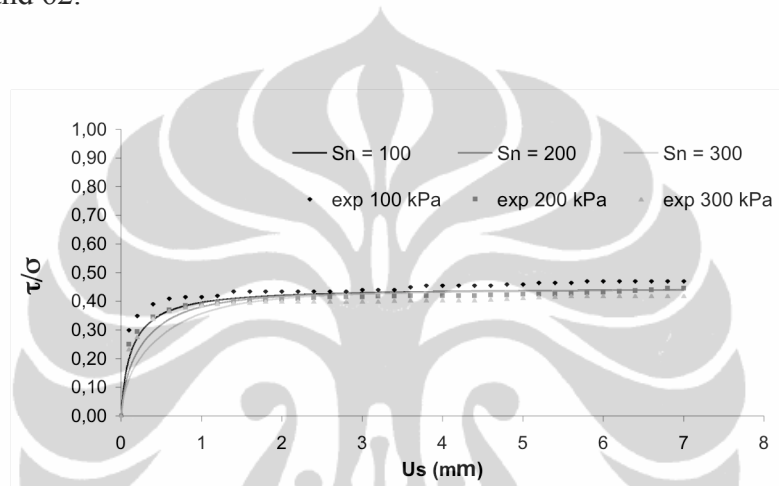


**Figure 61. Result of the simulation for a smooth interface and a loose sand (ID=15%) : stress ration curve**

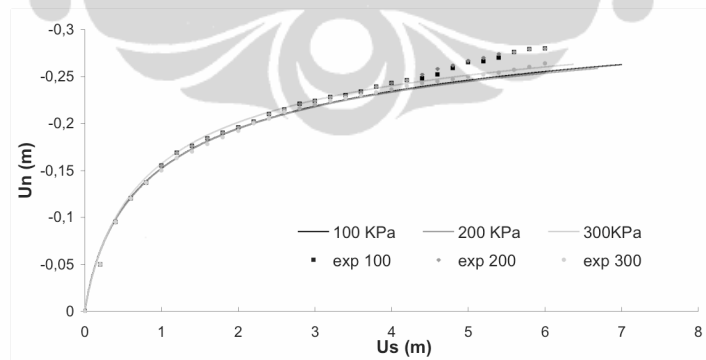


**Figure 62. Result of the simulation for a smooth interface and a loose sand (ID=15%): Displacement curve**

Through these two curves, it can be concluded that the proposed model, simulate correctly the behaviour of smooth interface with loose sand.

However, as regards the displacement curve, a phenomenon of second contractancy may also be observed. This phenomenon was not taken into account in modeling.

**VI.2. RESULTS OF CYCLICS SIMULATIONS**

The list of parameters used in the simulation during cyclic loading is provided in Table 6.

**Table 6. Cyclic model parameters**

	Type d'interface : Type de sand :	Rough		Smooth		Note
		Dense	Loose	Dense	Loose	
Ramberg Osgood model's parameters						
7	$\alpha$	0,5	0,5	-1	-1	
8	$r$	-0,5	-0,5	0,5	0,5	
Byrne law's parameters						
9	$C_1$	-0,09	-0,2	-0,022	-0,2	Deducted from the experimental result of Shahrou and Rezaie (1997)
10	$C_2$	-0,85	-0,85	-2	-2	Deducted from the experimental result of Shahrou and Rezaie (1997)

**VI.2.1. Shear stress curve**

Figures 63 to 66 present the results of the simulations of a cyclic solicitation. With these curves, we could conclude that there is a good reproduction of hysteresis loops by using the Ramberg-Osgood law, especially for simulation on a smooth interface, but a little less good for simulations carried out on a rough interface .

Hysteresis loops for rough interfaces, demonstrate clearly that the model based on the Ramberg-Osgood law greatly overestimates the surface of the hysteresis loop, especially during loading. This is probably due to the loop symmetry imposed by the criterion of Mohr-Coulomb.

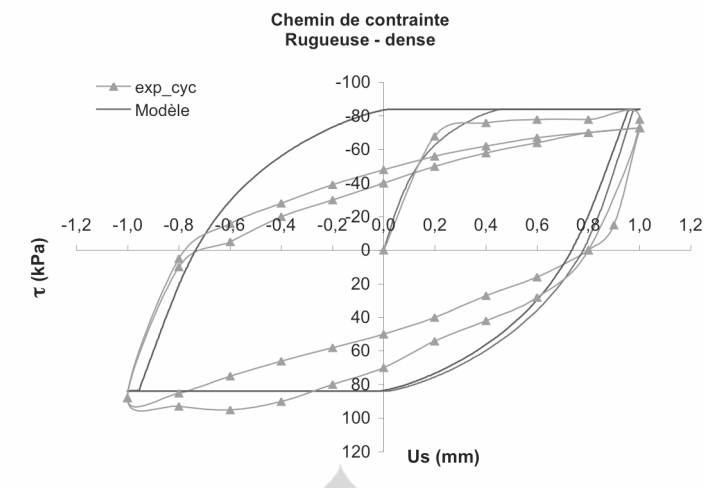


Figure 63. Shear stress curve for a rough interface with dense sand ( $ID=90\%$ ), during cyclic loading ( $\sigma_{n0} = 100$  kPa).

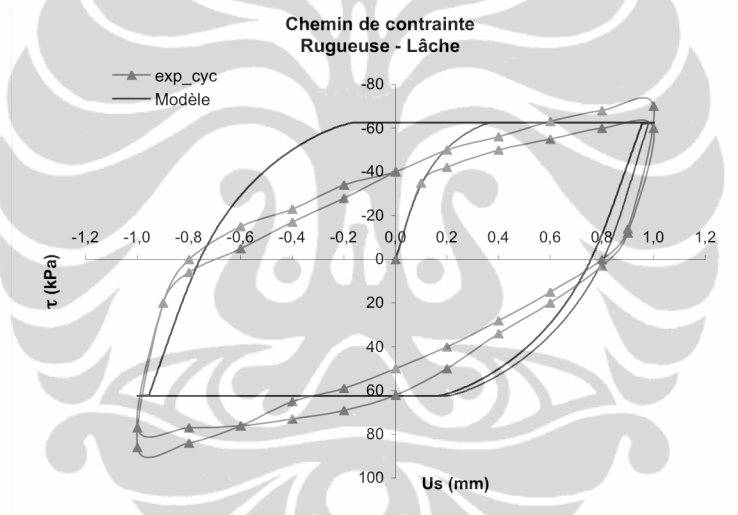


Figure 64. Shear stress curve for a rough interface with loose sand ( $ID=15\%$ ), during cyclic loading ( $\sigma_{n0} = 100$  kPa).

During cyclic loading, the interface normally stabilize it self after a certain amount of time. This stabilization could introduces a decrease or an increase of shear strength (softening or hardening) which could take place during the first loading-unloading that can be observed on the experimental hysteresis loop. According to the results of the simulation for a smooth interface, it is clear that there are no densification or stabilization which has occurred during the first few times. The model proposed in this study is therefore, not able to model this phenomenon.

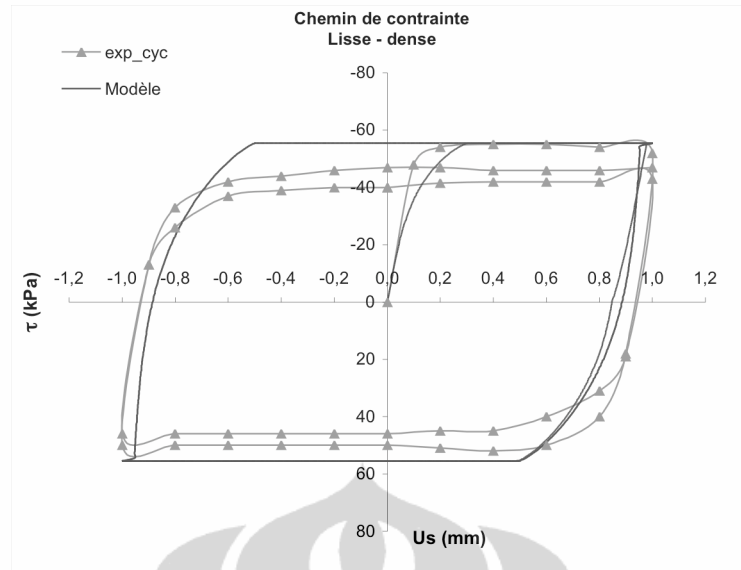


Figure 65. Shear stress curve for a smooth interface with dense sand ( $ID=90\%$ ), during a cyclic loading ( $\sigma_{n0} = 100$  kPa).

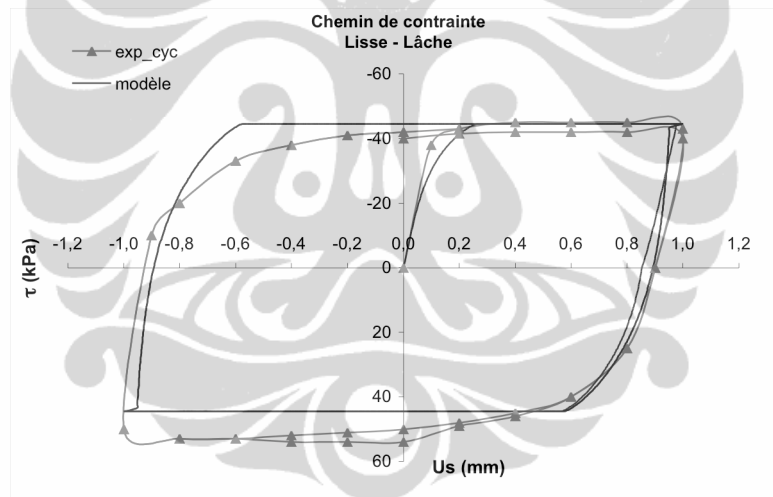


Figure 66. Shear stress curve for a smooth interface with loose sand ( $ID=15\%$ ), during a cyclic loading ( $\sigma_{n0} = 100$  kPa).

### VI.2.2. Displacement curve

Figures 67 to 70 show the displacement curves during cyclic loading on an interface. Usually after 20 cycles, the model proposed corresponds well with the experimental results. We can observe, however, on certain tests, some differences between the model and the experimental results at the beginning of the load.

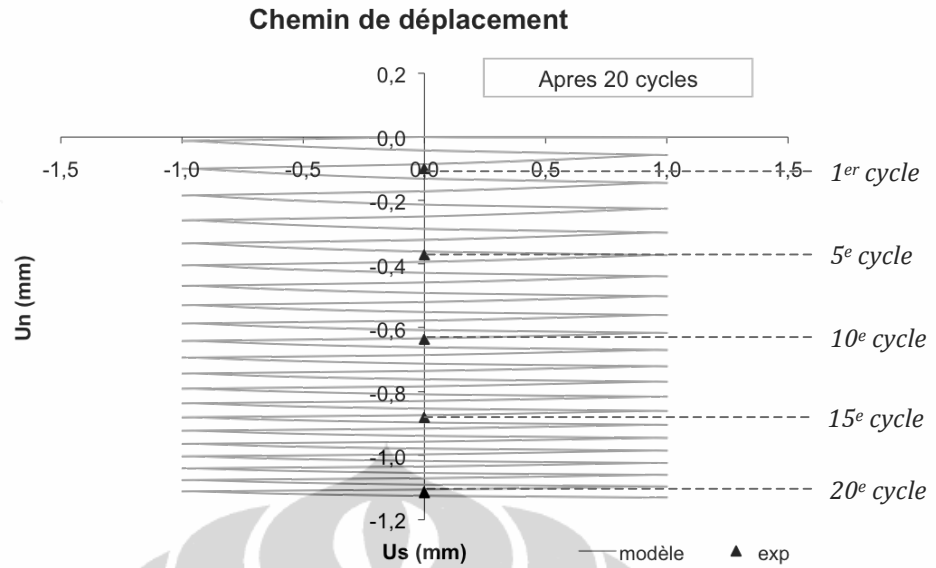


Figure 67. Displacement curve for a rough interface with dense sand ( $ID=90\%$ ), during cyclic loading ( $\sigma_{n0} = 100$  kPa).

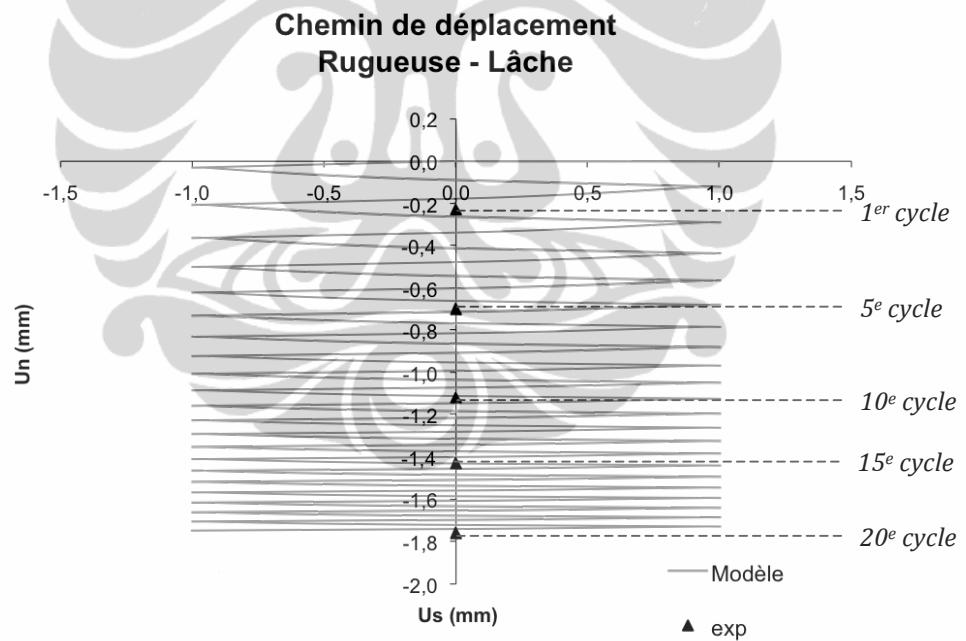


Figure 68. Displacement curve for a rough interface with loose sand ( $ID=15\%$ ), during cyclic loading ( $\sigma_{n0} = 100$  kPa).

The displacement curve for a rough interface with loose sand makes it more clear to be observed, that the model does not properly simulate the normal displacement at the beginning of the load (until 4th or 6th cycles). This phenomenon is

probably due to the chosen parameters of the Byrne law,  $C_1$  and  $C_2$ . Byrne curves for each type of interface tests are given in appendix F.

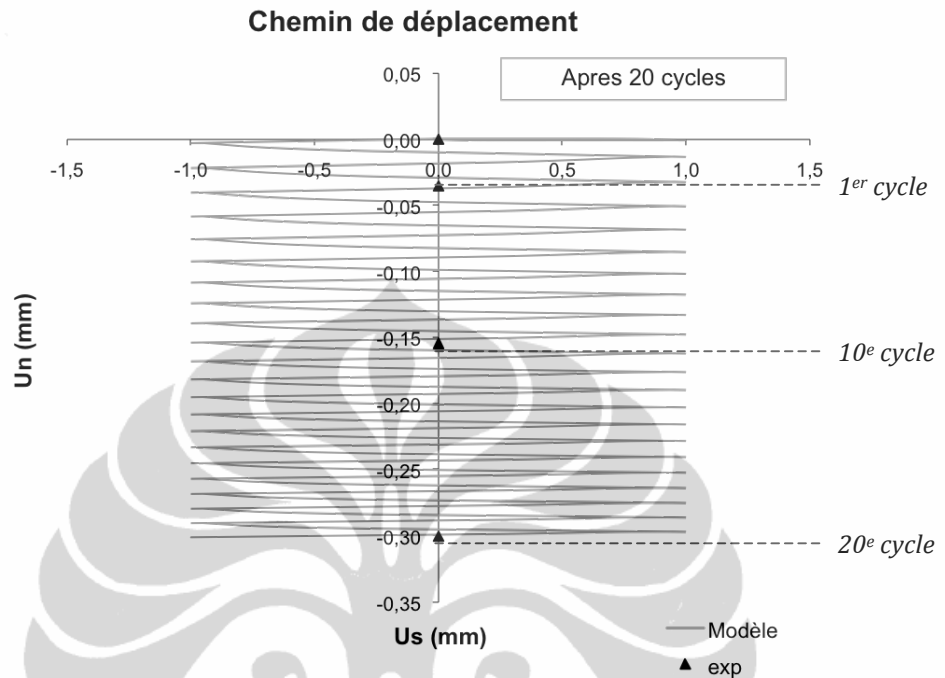


Figure 69. Displacement curve for a smooth interface with dense sand ( $ID=90\%$ ), during cyclic loading ( $\sigma_{n0} = 100$  kPa).

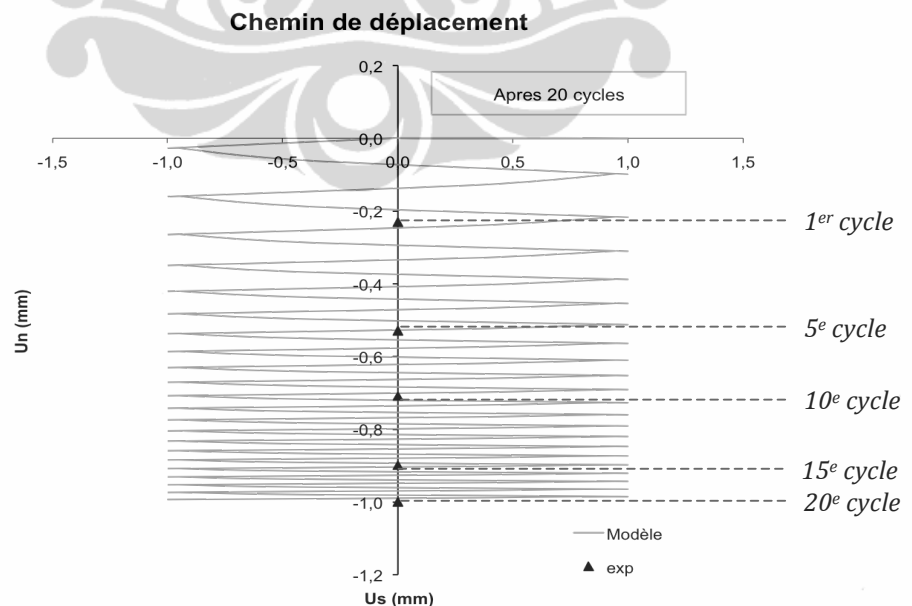


Figure 70. Displacement curve for a smooth interface with loose sand ( $ID=15\%$ ), during cyclic loading ( $\sigma_{n0} = 100$  kPa).

### ***VI.3. PARTIAL CONCLUSION***

Through these results it can be concluded that the proposed model correctly, despite some differences, the overall behaviour of the interface, including the phenomena of shear stress softening and contractors dilatancy during a monotonic solicitation, as well as the hysteresis loop during cyclic loading. Nevertheless, the results for an interface with a loose sand during a solicitation monotone, and the normal displacement obtained after N cycles are relatively close to the experimental results.

However, some important points remain unanswered. It has been particularly testify during this particularly studies the difficulty to determine the characteristics state's friction angle and maximum state parameter for interfaces with dense sand. An observation was also made on the stress ratio when tested on the same type of interface. The stress ratio of the simulation on an interface with a confinement that exceeds 100 kPa seems much less rigid compared to the experimentally obtained. All these observations suggest that the parameters  $\phi_{car}$ ,  $\phi_{max}$  and the softening model are influenced by the initial normal stress.

Regarding the cyclic simulation, it can be concluded that the criterion of Mohr-Coulomb alone is not sufficient to take into account the hardening or softening of hysteresis loops. This model based on the law of Ramberg-Osgood and the law of Byrne remains to be modified or completed to better model the cyclical behaviour of the interface.